Hypoxia-Induced MIF Induces Dysregulation of Lipid Metabolism in Laryngocarcinoma Through IL-6/JAK-STAT Pathway

Minlan Yang (yangml@whu.edu.cn)
Zhongnan hospital of Wuhan University
Sa Wu
Zhongnan hospital of Wuhan University
Weisong Cai
Zhongnan hospital of Wuhan University
Xiaoping Ming
Zhongnan hospital of Wuhan University
Yuhao Zhou
Zhongnan hospital of Wuhan University
Xiong Chen
Zhongnan hospital of Wuhan University

Research Article

Keywords: hypoxia, MIF, lipid metabolism, IL-6/JAK-STAT pathway

Posted Date: March 16th, 2022

DOI: https://doi.org/10.21203/rs.3.rs-1439230/v1

Abstract

Purpose

Hypoxia is a common feature of laryngocarcinoma. Alteration in lipid metabolism in hypoxic microenvironment is an important metabolic rewiring phenomenon for malignant cells to maintain their rapid proliferation, which makes most cancers, including laryngocarcinoma, hard to cure. However, the mechanism of lipid metabolism of laryngocarcinoma involved is still unclear. This study aimed to make clear the changes in lipid metabolism of laryngocarcinoma cell under hypoxic condition and explore the relative mechanism.

Methods

Hep2 cells were placed in a normoxic or hypoxic environment (5% CO2, 94% N2 and 1% O2) at 37°C for 24 h. After exposed to hypoxia, lip metabolic indices including TG and NEFA were tested. The mechanism involved in lip metabolism regulation was explored by RNA seq and bioinformatic analysis. MIF inhibitor ISO-1 and JAK inhibitor XL019 were used to verify the mechanism. Finally, tumour xenograft model was applied has further verified these results in vivo.

Results

Hypoxia increased the TG and NEFA levels of Hep2 cells. Three genes, intersection of hypoxia gene sets and fatty gene sets, including MIF, ENO2, and LDHA were screened and verified by qPCR. MIF levels were elevated when exposed to hypoxia. Through GSEA and RNA-seq analysis, JAK/STAT pathway was screened. Hypoxia increased MIF and activated IL-6/JAK/STAT pathway. MIF inhibitor ISO-1 reversed TG levels, IL-6 levels, and reversed the expression pattern of screened genes in JAK/STAT pathway. Tumour xenograft model has further verified these results.

Conclusion

Hypoxia induced reprogramming of lipid metabolism in laryngocarcinoma cells through MIF/IL-6/JAK-STAT pathway. This study revealed one mechanism that allows laryngocarcinoma cells adapt to hypoxic tumor microenvironment. Therefore, a drug targeting MIF/IL-6/JAK-STAT pathway might be a promising therapeutic option for the treatment of laryngeal cancer.

Introduction

Hypoxia is a common phenomenon in the tumor microenvironment. In the process of tumor progression, due to the rapid proliferation of tumor cells, the vascular network cannot be established quickly and the new blood vessels are structurally abnormal, resulting in a decrease in oxygen content in the microenvironment, lack of nutrients and accumulation of acidic substances. In the hypoxic microenvironment, tumor cells can improve their adaptability by changing ways of metabolism, inhibiting the anti-tumor effects of immune cells, prone to invasion, metastasis, and drug-resistance. Therefore, the hypoxic microenvironment increases the difficulty of tumor treatment. Lipids, proteins, and nucleic acids are important components of the biological membranes and structural units of cells. Lipids are used for energy storage and metabolism and play important signaling molecular roles in a variety of cellular activities. The regulation of lipid metabolism, such as lipid uptake, synthesis, and hydrolysis, is essential for maintaining cell homeostasis. In the process of tumor progression, the availability of nutrients in the tumor microenvironment is constantly changing, tumor cells undergo lipid metabolism to maintain rapid proliferation, survival, migration, invasion, and metastasis. To adapt to the hypoxic microenvironment, the metabolism of tumors will also undergo corresponding changes. Hypoxia enhances lipogenesis by HIF-dependent modulation of proteins involved in fatty acid (FA) uptake, synthesis, storage and usage, enhancing cancer progression and hypoxia-induced chemoresistance[1–3]. Hypoxia-induced alteration of lipid metabolism promotes cancer malignant progression has been explored in various cancers.

In prostate cancer, hypoxic cells accumulate a higher amount of lipids and decreased fatty acid oxidation, protecting cancer cells from oxidative and endoplasmic reticulum stress, and playing important roles in fueling cell proliferation[4]. In clear cell renal cell carcinoma (ccRCC), HIF1 and HIF2 repressed target gene CPT1A, thus reducing fatty acid transport into the mitochondria, and forcing fatty acids to lipid droplets for storage, which is essential for ccRCC tumorigenesis[5]. In a hypoxic microenvironment, HIF-2α upregulation promotes steatotic hepatocellular carcinoma progression by activating lipid synthesis via the PI3K-AKT-mTOR pathway[6]. Inhibition of lipid storage decreased the survival of cells subjected to hypoxia-reoxygenation and strongly impaired tumorigenesis in multiple cancers[7]. As laryngeal cancer is a common disease in otorhinolaryngology, and with increasing incidence rate in recent years. We aim to explore the role of hypoxia in the lipid metabolism in laryngeal cancer cells in this study.

Methods And Materials

1. Cell culture

A human laryngeal squamous cancer cell line, Hep2, was purchased from Medical Science Research Center, Zhongnan Hospital of Wuhan University, and cultured in Dulbecco's modified Eagle's medium supplemented with 10% fetal bovine serum, 100U/ml penicillin and 100μg/ml streptomycin. Cells were maintained at 37℃ in a humidified incubator with a mixture of 95% air (20% O_2) and 5% CO_2. 1%O_2, 94%N2 and 5%CO_2 was chosen for hypoxia experiment. MIF inhibitor ISO-1 (SML0472) was purchased from Sigma-Aldrich, and JAK inhibitor XL019 was purchased from Beyotime Biotechnology.

2. Western blotting

For Western blotting, cells were lysed with RIPA lysis buffer kit (Beyotime, China), supernatants were collected after spin and total proteins were measured using the BCA protein quantification kit (Beyotime, China). Total protein samples were separated by 10% sodium dodecyl sulphate polyacrylamide gel electrophoresis (SDS-PAGE). Then, the samples were transferred onto 0.22μm PVDF membranes. After blocking with 5% fat-free milk for 1 hour at room temperature, the membranes were incubated with primary antibodies overnight at 4℃. Following three washes with TBST buffer, the membranes were incubated with secondary goat anti-rabbit antibodies conjugated with HRP for 1 hour at room temperature. Signals were visualized using the enhanced chemiluminescence kit (Beyotime, China) and detected by the Imaging system (Baygene Biotech, China). Integrated relative densities of individual bands were quantified using Image J (National Institutes of Health, Bethesda, MD).

3. Quantitative real-time PCR

Total RNA was extracted following the manufacturer's protocol with TRIzol reagent (Invitrogen, CA), dissolved in RNA-free H_2O and stored at -80°C. cDNA synthesis was performed from each 1μg RNA sample using the Reverse Transcriptase Kit (Thermo, USA). Then qRT-PCR was performed on a CFX96 Connect (Bio-Rad, CA) using a SYBR Green PCR kit (Vazyme Biotech, China). Expression data were calculated using the $2^{-\Delta\Delta Ct}$ method and normalized by taking GAPDH as an internal reference to control the relative expression levels. Primer sequences were listed in Table 1.

4. ELISA assay

MIF and IL-6 concentrations were detected by enzyme-linked immunosorbent assay (ELISA) kits according to the manufacturer's protocol. Quantitative IL-6 ELISA assay kit was purchased from QuantiCyto (China), Quantitative MIF ELISA assay kit was purchased from Elabscience (USA), and TG, NEFA levels were estimated by assay kits (Nanjing Jiancheng Bioengineering Institute, China). All were used according to the manufacturers' instructions. All samples were measured in triplicate and average values were determined.

5. Bioinformatics analysis

Hypoxia gene sets and fatty gene sets were downloaded from Gene Set Enrichment Analysis(GSEA, http://www.gsea-msigdb.org/gsea/index.jsp) and Venn diagrams were used to analyze the intersection of the two gene sets. Gene expression profiles of larynx were downloaded from TCGA (https://portal.gdc.cancer.gov/). Gene Set Enrichment Analysis (GSEA) was performed using GSEA software 4.0.3(USA).

6. RNA-seq

Transcriptome sequencing and analysis were performed by the BGI Company (http://bgitechsolutions.com). Total RNA was extracted following the manufacturer's protocol with TRIzol reagent (Invitrogen, CA), dissolved in RNA-free H_2O and stored at -80°C. Total RNA was processed by mRNA enrichment: The mRNA with polyA tail was enriched by magnetic beads with OligodT. The RNA obtained was segmented by interrupting buffer, and the random N6 primers were reversely transcribed, and then the cDNA two-strand was synthesized to form double-stranded DNA. The synthetic double-stranded DNA ends are flattened and phosphorylated at the 5' end to form A sticky end protruding an "A" at the 3' end, followed by A bubbling-like connector protruding A "T" at the 3' end. The ligands were amplified by PCR using specific primers. The PCR product was thermally denatured into single strand, and then the single strand DNA was cycled with a bridge primer to obtain a single strand circular DNA library. The constructed library was inspected and sequenced after qualified. The resulting data are referred to as RAW reads or RAW data, and the RAW reads are then subjected to quality control (QC) to determine whether the sequenced data are suitable for subsequent analysis. After quality control, the filtered clean reads were compared to the reference sequence. After alignment, the distribution of alignment rate and reads on the reference sequence was counted to determine whether alignment results passed the second QC of alignment. If passed, gene quantitative analysis was carried out and differential gene expression among screened samples will be conducted.

7. Immunohistochemistry staining

Tissue slides were deparaffinized in xylene and rehydrated in alcohol. Then, antigen retrieval was performed with 0.1 M sodium citrate buffer. Subsequently, the sections were blocked by performing IHC kit(Maixin China) and probed with primary antibodies for 1 h at room temperature. Slides were incubated with poly-HRP secondary antibodies by performing IHC kit, after which sections were counterstained with haematoxylin to visualize nuclei. Images were analyzed by using Image J v1.8.0(National Institutes of Health, USA).

8. Animal experiment

All mice were maintained at Zhongnan Hospital of Wuhan University and all animal experiments were performed in accordance with Zhongnan Hospital animal ethics committee(Wuhan, China). Male BABL/c nude mice (4 weeks old) were purchased from Gempharmatech (Zhejiang, China). Hep2 cells were resuspended at 2×10^7 cells/mL using saline, and each mouse was subcutaneously injected 200 μL into the right anterior flank. After 8 days, the mice were randomly divided into treatment group and control group(5 mice per group). The treatment group was treated with ISO-1(2.5 mg/kg, intraperitoneally, every day) and the control group was treated with saline(equal volume per weight, intraperitoneally, every day). Tumor volume was measured using a caliper every other day, and volumes were calculated using the standard formula: $V = 0.5*length*width^2$. Finally, mice were euthanized, and tumors were removed, photographed, weighed and collected for ELISA and immunohistochemistry.

9. Statistical analysis

All data were represented as means ± standard deviations (SD). All differences between two independent groups were analyzed using Students' t test. SPSS 20.0 software (IBM Corporation, USA) was used for statistical analysis. A P-value < 0.05 was considered statistically significant.

Results

Hypoxia affects lipid metabolism in Hep2 cells

Hypoxia inducible factor 1 subunit alpha (HIF1A), which is an adaptive factor in the hypoxic environment, was found higher expressed when Hep2 cells exposed hypoxic environment as 1% O_2(Fig. 1A). To make sure whether hypoxia affects HNSCC lipid metabolism, Triglycerides (TG), which is a constituent of lipids, were detected. We found that hypoxia evidently increased the TG level of Hep2 cells(Fig. 1B). Besides, non-esterified free fatty acids (NEFA) are the major component of triglycerides, we also found that hypoxia increased NEFA level in Hep2 cells(Fig. 1C). Furthermore, we found that the expression pattern of some lipid metabolism related genes was changed, the expressions of PPARA, PPARG, SREBF1, FASN, PPARD were downregulated, and LPIN2 was upregulated when exposed to hypoxia(Fig. 1D). According to these findings, it suggested that hypoxia may make a role in regulating lipid metabolism in HNSCC cells.

MIF may be a key factor in hypoxia regulating lipid metabolism

As hypoxia is a common feature of solid tumors, cancer cells confront the compound challenges of high growth rates and limited and unreliable supply of O_2, therefore cancer cells change the pattern of metabolism to adapt to hyperproliferation. To explore whether lipid metabolism is involved when laryngeal cancer exposed to hypoxia microenvironment, we analyzed the hypoxia gene sets and fatty gene sets, three genes such as Lactate dehydrogenase A (LDHA), enolase 2 (ENO2) and macrophage migration inhibitory factor (MIF) may be involved in lipid metabolism in laryngeal cancer(Fig. 2A). In consistent with the intersection of the hypoxia gene sets and fatty gene sets by bioinformatics analysis, hypoxia significantly upregulated the expression of LDHA, ENO2 and MIF(Fig. 2B). As MIF is a classical pro-inflammatory cytokine that is secreted by immune cells and certain other cell types, we found that the protein level of MIF is increased when exposed to hypoxia. Since MIF is also a key factor in lipid metabolism disturbance, we hypothesized that MIF signaling may play a great role in hypoxia-inducing lipid metabolic disorder. To verify whether MIF is the main factor in hypoxia affecting lipid metabolism, ISO-1, a MIF antagonist was used. We found that 25μM ISO-1 significantly inhibited the protein level of MIF, and in the condition of hypoxic environment(Fig. 2C,2D), ISO-1 evidently decreased the TG level of Hep2 cells ($P < 0.01$)(Fig. 2E), and NEFA level of Hep2 cells is slightly decreased, though the statistical analysis showed no difference ($P > 0.05$)(Fig. 2F). To further verify the role of MIF in lipid metabolism, we found that ISO-1 reversed the expression of lipid metabolism related genes(Fig. 2G).

JAK/STAT signaling is involved in MIF regulating pathways in laryngeal cancer

GSEA analysis was used to screen the pathways which are involved in MIF regulating pathways in laryngeal cancer(Gene sets enriched in phenotype l (251 samples)), we found that the top 10 pathways were JAK STAT SIGNALING PATHWAY, ADHERENS JUNCTION, ARRHYTHMOGENIC RIGHT VENTRICULAR CARDIOMYOPATHY ARVC, ECM RECEPTOR INTERACTION, HUNTINGTONS DISEASE, ALZHEIMERS DISEASE, OXIDATIVE PHOSPHORYLATION, PARKINSONS DISEASE, GLUTATHIONE METABOLISM and SPLICEOSOME(Table.1). MIF was an upstream modulator of IL-6 and the IL-6/JAK/STAT pathway has a key role in the growth and development of many human cancers. Thence we hypothesized that hypoxia inducing MIF regulating lipid metabolism may through activating IL-6/JAK/STAT signaling(Fig. 3A). 14 genes were found to be consistent by the intersection of JAK/STAT pathway gene sets and RNA-seq(Fig. 3B). RT-qPCR was used to verify and the gene expression profile is basically consistent with the analysis(Fig. 3C), confirming that hypoxia activated JAK/STAT signaling pathway.

Hypoxia induces MIF regulating lipid metabolism through activating IL-6/JAK/STAT signaling

When exposed to hypoxia, the mRNA and protein levels of IL-6 were increased(Fig. 4A,4B). ISO-1 significantly reversed hypoxia inducing IL-6 upregulation(Fig. 4C,4D). RT-qPCR assay was applied to test the mRNA expression of JAK/STAT pathway genes, it revealed that ISO-1 reversed the expression pattern of JAK/STAT pathway genes profile, suggesting hypoxia activating IL-6/JAK/STAT pathway via MIF(Fig. 4E). To further verify that MIF regulating lipid metabolism through activating IL-6/JAK/STAT pathway, JAK inhibitor XL019 was used, we found that XL019 significantly decreased the TG level of Hep2

cells when exposed to hypoxia(Fig. 4F), it confirmed that inhibition of JAK signaling reversed hypoxia inducing abnormal lipid metabolism.

MIF antagonist ISO1 inhibits the tumorigenicity of Hep2 cells in vivo

To evaluate whether MIF plays a role in tumorigenicity in vivo, we applied ISO1, a MIF antagonist, to tumor-bearing mice. ISO1 significantly inhabited the tumor growth in vivo(Fig. 5A). Tumor weight(Fig. 5B) obviously decreased in mice injected with ISO1 compared with control mice. Furthermore, the positive rate of Ki67, which reflects the proliferation of cells, was obviously lower in the ISO1 treatment group(Fig. 5C). In inconsistent with the results of cell experiment, the concentration of serum IL6(Fig. 5D) and serum TG(Fig. 5E) was decreased with ISO1 treatment. To explore the mechanism of cancer cells adapting to hypoxic microenvironment, we conducted RT-qPCR assay to test the mRNA expression of JAK/STAT pathway genes of tumor xenograft tissues. The results were basically accordance with the cellular data(Fig. 5F). In summary, all these results suggest that hypoxia activated IL-6/JAK/STAT pathway via MIF.

Discussion

Lipids, proteins and nucleic acids are important components of the biological membranes and structure of cells. In addition, lipids are also used for energy storage and metabolism and play important signaling molecular roles in a variety of cellular activities. The regulation of lipid metabolism, such as lipid uptake, synthesis, and hydrolysis, is essential for maintaining cell homeostasis. In the process of tumor progression, the availability of nutrients in the tumor microenvironment is constantly changing, tumor cells alter lipid metabolism to maintain rapid proliferation, survival, metastasis and chemoresistance.

Under hypoxic conditions, cancer cells increase the utilization of extracellular lipids to meet the demand for bioenergy and biosynthesis and to maintain membrane homeostasis. Fatty acid metabolism maintains tumorigenesis, progression and treatment resistance by enhancing lipid synthesis, storage and catabolism. In addition, tumor cells exhibit plasticity in fatty acid metabolism and respond to extraneous and systemic metabolic signals (such as obesity and tumor therapy) to promote aggressiveness, treatment and resistance to the development of related diseases[8]. In our study, we found that hypoxia increased TG and NEFA levels in Hep2 cells, and then we screened the fat acid metabolism related genes in hypoxia gene sets of laryngeal cancer. MIF, ENO2 and LDHA were screened as related to lipid metabolism when laryngeal cancer cells exposed to hypoxia, which is consistent with the RNA-seq analysis of Hep2 cells that exposed to hypoxia. MIF is over-expressed and secreted in various cancer cells in particular in response to hypoxia. As a multifunctional inflammatory cytokine, MIF is related to tumorigenesis, angiogenesis and metastasis of many cancer phenotypes. MIF can potentially promote tumorigenesis by inhibiting the classic tumor suppressor gene p53, regulating cell cycle arrest and apoptosis in response to DNA damage[9]. Besides, inhibition of MIF can reduce the formation of the pre-metastasis microenvironment in the liver and the metastasis of cancer cells[10].

In recent years, MIF was reported associated with lipid metabolism in multiple diseases. Changes in expression levels of MIF have an important impact on metabolism and immune regulation of adipose cells. MIF deficiency aggravates the effects of energy-rich fructose diet on hepatic lipid accumulation in the mouse liver[11]. MIF upregulation reduced lipolysis and increased lipogenic pathways in adipose tissue[12]. MIF deficiency reduces chronic inflammation in white adipose tissue[13]. We verified that hypoxia inducing increased TG and NEFA levels via upregulating of MIF by antagonist, ISO-1. And ISO-1 reversed the expression pattern of lipid metabolism related genes, such as PPARA, PPARG, SREBF1, FASN, LPIN2. Through subcutaneous xenograft model, we found that tumors was significantly growth-restricted with ISO-1 treatment. Consistently, the serum IL6 and TG levels of mice showed the same trend. However, there were no statistically significant differences possibly due to large individual variations. More mice are needed for a reliable conclusion.

Besides the key role of MIF on the inflammatory cascade and its ability to counteract glucocorticoid-induced anti-inflammatory responses, MIF also participates in regulating malignant phenotypes of various cancers through activating multiple signaling pathways. MIF expression is abnormally increased and supports the proliferation, migration and invasion of breast cancer, gastric cancer, pancreatic cancer and lung cancer cells[14–17]. MIF acts as an autocrine growth factor

involved in cell cycle in pancreatic cancer cells[18]. In bladder cancer cells, activation of CXCL2/MIF-CXCR2 signaling induced MDSC accumulation and expansion in the bladder cancer microenvironment[19]. MIF/CXCR7/AKT pathway drives growth and metastasis in castration-resistant prostate cancer cells[20].

To further analyze the molecular mechanism of MIF in regulating lipid metabolism, we screened the related pathway through GSEA analysis, and we found the top one pathway is JAK/STAT pathway. Through the intersection of JAK/STAT pathway gene sets and RNA-seq, we screened that 14 genes showed the same expression patterns, and RT-qPCR results basically verified it in vitro and in vivo. Due to large individual variations of each mouse, a part of genes did not show a siganificant difference even though the trend of gene expression in vivo was consistent with the results in vitro. As MIF was an upstream modulator of IL-6, and IL-6 is the classical upstream activator of JAK/STAT pathway, IL-6 binds to its receptor IL-6R, and induces homodimerization and formation of a high affinity receptor complex, activating MAPK, PI3K/AKT pathways, to regulate growth, differentiation, survival and chemoresistance of cancer cells[21–23].

JAK/STAT signaling pathway is continuously activated and overexpressed in a variety of tumor cells, the continuously activated JAK/STAT pathway in the tumor microenvironment can inhibit the anti-tumor immune response of immune cells, IL-6/JAK/STAT signal has become a hot signal target for tumor therapy[24]. MIF promotes the secretion of the inflammatory factor IL-6 in the tumor hypoxic microenvironment, and promotes the malignant progression of laryngeal cancer and changes in lipid metabolism, suggesting that MIF/IL-6/JAK/STAT pathway is expected to provide a new approach for the treatment of laryngeal cancer.

Abbreviations

HNSCC
head and neck squamous cell carcinoma
ELISA
enzyme-linked immunosorbent assay
GSEA
gene set enrichment analysis
IHC
immunohistochemistry
NEFA
non-esterified free fatty acids
FA
fatty acid
TG
triglycerides
HIF1A
hypoxia inducible factor 1 subunit alpha
MIF
macrophage migration inhibitory factor
LDHA
lactate dehydrogenase A
ENO2
enolase 2

Declarations

Ethics approval

The animal study was reviewed and approved by the Ethics Committee of Zhongnan Hospital of Wuhan University.

Consent for publication

Not applicable

Availability of data and materials

The following information was supplied regarding data availability: The gene expression profiles containing the clinical follow-up information is available at TCGA website(https://www.cancer.gov/about-nci/organization/ccg/research/structural-genomics/tcga). The other data used to support the findings of this study are available from the corresponding author upon request.

Competing Interests

The authors have no relevant financial or non-financial interests to disclose.

Funding

This work was partly supported by the National Natural Science Foundation of China (NO. 81902599).

Author Contributions

Minlan Yang: Conceptualization, Methodology, Validation, Formal analysis, Investigation, Data Curation, Writing-Original Draft. Sa Wu: Conceptualization, Methodology, Validation, Formal analysis, Investigation, Data Curation, Writing-Original Draft. Weisong Cai: Methodology, Validation, Software, Formal analysis, Investigation, Data Curation, Writing-Original Draft. Xiaoping Ming: Resources, Data Curation. Yuhao Zhou: Data Curation, Visualization. Xiong Chen: Writing- Review & Editing, Supervision. All authors have participated sufficiently in the study and approved the final version

Data Availability

The following information was supplied regarding data availability: The gene expression profiles containing the clinical follow-up information is available at TCGA website(https://www.cancer.gov/about-nci/organization/ccg/research/structural-genomics/tcga). The other data used to support the findings of this study are available from the corresponding author upon request.

Acknowledgements

Not applicable

References

1. C. Corbet, O. Feron, Emerging roles of lipid metabolism in cancer progression, Curr Opin Clin Nutr Metab Care, 20 (2017) 254–260, https://doi.org/10.1097/MCO.0000000000000381.
2. X. Luo, C. Cheng, Z. Tan, N. Li, M. Tang, L. Yang, Y. Cao, Emerging roles of lipid metabolism in cancer metastasis, Mol Cancer, 16 (2017) 76, https://doi.org/10.1186/s12943-017-0646-3.
3. I. Mylonis, G. Simos, E. Paraskeva, Hypoxia-Inducible Factors and the Regulation of Lipid Metabolism, Cells-Basel, 8 (2019), https://doi.org/10.3390/cells8030214.
4. G. Deep, I.R. Schlaepfer, Aberrant Lipid Metabolism Promotes Prostate Cancer: Role in Cell Survival under Hypoxia and Extracellular Vesicles Biogenesis, Int J Mol Sci, 17 (2016), https://doi.org/10.3390/ijms17071061.
5. Du W, L. Zhang, A. Brett-Morris, B. Aguila, J. Kerner, C.L. Hoppel, M. Puchowicz, D. Serra, L. Herrero, B.I. Rini, S. Campbell, S.M. Welford, HIF drives lipid deposition and cancer in ccRCC via repression of fatty acid metabolism, Nat Commun, 8

(2017) 1769, https://doi.org/10.1038/s41467-017-01965-8.

6. J. Chen, J. Chen, J. Huang, Z. Li, Y. Gong, B. Zou, X. Liu, L. Ding, P. Li, Z. Zhu, B. Zhang, H. Guo, C. Cai, J. Li, HIF-2α upregulation mediated by hypoxia promotes NAFLD-HCC progression by activating lipid synthesis via the PI3K-AKT-mTOR pathway, Aging (Albany NY), 11 (2019) 10839–10860, https://doi.org/10.18632/aging.102488.
7. K. Bensaad, E. Favaro, C.A. Lewis, B. Peck, S. Lord, J.M. Collins, K.E. Pinnick, S. Wigfield, F.M. Buffa, J.L. Li, Q. Zhang, M. Wakelam, F. Karpe, A. Schulze, A.L. Harris, Fatty acid uptake and lipid storage induced by HIF-1α contribute to cell growth and survival after hypoxia-reoxygenation, Cell Rep, 9 (2014) 349–365, https://doi.org/10.1016/j.celrep.2014.08.056.
8. Y. Cao, Adipocyte and lipid metabolism in cancer drug resistance, J Clin Invest, 129 (2019) 3006–3017, https://doi.org/10.1172/JCI127201.
9. C. O'Reilly, M. Doroudian, L. Mawhinney, S.C. Donnelly, Targeting MIF in Cancer: Therapeutic Strategies, Current Developments, and Future Opportunities, Med Res Rev, 36 (2016) 440 – 60, https://doi.org/10.1002/med.21385.
10. B. Costa-Silva, N.M. Aiello, A.J. Ocean, S. Singh, H. Zhang, B.K. Thakur, A. Becker, A. Hoshino, M.T. Mark, H. Molina, J. Xiang, T. Zhang, T.M. Theilen, G. García-Santos, C. Williams, Y. Ararso, Y. Huang, G. Rodrigues, T.L. Shen, K.J. Labori, I.M. Lothe, E.H. Kure, J. Hernandez, A. Doussot, S.H. Ebbesen, P.M. Grandgenett, M.A. Hollingsworth, M. Jain, K. Mallya, S.K. Batra, W.R. Jarnagin, R.E. Schwartz, I. Matei, H. Peinado, B.Z. Stanger, J. Bromberg, D. Lyden, Pancreatic cancer exosomes initiate pre-metastatic niche formation in the liver, Nat Cell Biol, 17 (2015) 816 – 26, https://doi.org/10.1038/ncb3169.
11. L. Gligorovska, A. Teofilović, M.D. Vojnović, N. Miladinović, S. Kovačević, N. Veličković, A. Djordjevic, Macrophage migration inhibitory factor deficiency aggravates effects of fructose-enriched diet on lipid metabolism in the mouse liver, Biofactors, 47 (2021) 363–375, https://doi.org/10.1002/biof.1711.
12. D. Cui, Y. Peng, C. Zhang, Z. Li, Y. Su, Y. Qi, M. Xing, J. Li, G.E. Kim, K.N. Su, J. Xu, M. Wang, W. Ding, M. Piecychna, L. Leng, M. Hirasawa, K. Jiang, L. Young, Y. Xu, D. Qi, R. Bucala, Macrophage migration inhibitory factor mediates metabolic dysfunction induced by atypical antipsychotic therapy, J Clin Invest, 128 (2018) 4997–5007, https://doi.org/10.1172/JCI93090.
13. L. Verschuren, T. Kooistra, J. Bernhagen, P.J. Voshol, D.M. Ouwens, M. van Erk, D.W.J. de Vries-van, L. Leng, J.H. van Bockel, K.W. van Dijk, G. Fingerle-Rowson, R. Bucala, R. Kleemann, MIF deficiency reduces chronic inflammation in white adipose tissue and impairs the development of insulin resistance, glucose intolerance, and associated atherosclerotic disease, Circ Res, 105 (2009) 99–107, https://doi.org/10.1161/CIRCRESAHA.109.199166.
14. B. Cheng, Q. Wang, Y. Song, Y. Liu, Y. Liu, S. Yang, D. Li, Y. Zhang, C. Zhu, MIF inhibitor, ISO-1, attenuates human pancreatic cancer cell proliferation, migration and invasion in vitro, and suppresses xenograft tumour growth in vivo, Sci Rep, 10 (2020) 6741, https://doi.org/10.1038/s41598-020-63778-y.
15. X.X. He, J. Yang, Y.W. Ding, W. Liu, Q.Y. Shen, H.H. Xia, Increased epithelial and serum expression of macrophage migration inhibitory factor (MIF) in gastric cancer: potential role of MIF in gastric carcinogenesis, Gut, 55 (2006) 797–802, https://doi.org/10.1136/gut.2005.078113.
16. E. Verjans, E. Noetzel, N. Bektas, A.K. Schütz, H. Lue, B. Lennartz, A. Hartmann, E. Dahl, J. Bernhagen, Dual role of macrophage migration inhibitory factor (MIF) in human breast cancer, Bmc Cancer, 9 (2009) 230, https://doi.org/10.1186/1471-2407-9-230.
17. L. Mawhinney, M.E. Armstrong, R.C. O', R. Bucala, L. Leng, G. Fingerle-Rowson, D. Fayne, M.P. Keane, A. Tynan, L. Maher, G. Cooke, D. Lloyd, H. Conroy, S.C. Donnelly, Macrophage migration inhibitory factor (MIF) enzymatic activity and lung cancer, Mol Med, 20 (2015) 729 – 35, https://doi.org/10.2119/molmed.2014.00136.
18. A. Denz, C. Pilarsky, D. Muth, F. Rückert, H.D. Saeger, R. Grützmann, Inhibition of MIF leads to cell cycle arrest and apoptosis in pancreatic cancer cells, J Surg Res, 160 (2010) 29–34, https://doi.org/10.1016/j.jss.2009.03.048.
19. H. Zhang, Y.L. Ye, M.X. Li, S.B. Ye, W.R. Huang, T.T. Cai, J. He, J.Y. Peng, T.H. Duan, J. Cui, X.S. Zhang, F.J. Zhou, R.F. Wang, J. Li, CXCL2/MIF-CXCR2 signaling promotes the recruitment of myeloid-derived suppressor cells and is correlated with prognosis in bladder cancer, Oncogene, 36 (2017) 2095–2104, https://doi.org/10.1038/onc.2016.367.

20. S. Rafiei, B. Gui, J. Wu, X.S. Liu, A.S. Kibel, L. Jia, Targeting the MIF/CXCR7/AKT Signaling Pathway in Castration-Resistant Prostate Cancer, Mol Cancer Res, 17 (2019) 263–276, https://doi.org/10.1158/1541-7786.MCR-18-0412.
21. D.E. Johnson, R.A. O'Keefe, J.R. Grandis, Targeting the IL-6/JAK/STAT3 signalling axis in cancer, Nat Rev Clin Oncol, 15 (2018) 234–248, https://doi.org/10.1038/nrclinonc.2018.8.
22. P. Sansone, J. Bromberg, Targeting the interleukin-6/Jak/stat pathway in human malignancies, J Clin Oncol, 30 (2012) 1005–14, https://doi.org/10.1200/JCO.2010.31.8907.
23. J. Lokau, V. Schoeder, J. Haybaeck, C. Garbers, Jak-Stat Signaling Induced by Interleukin-6 Family Cytokines in Hepatocellular Carcinoma, Cancers (Basel), 11 (2019), https://doi.org/10.3390/cancers11111704.
24. C.S. Roxburgh, D.C. McMillan, Therapeutics targeting innate immune/inflammatory responses through the interleukin-6/JAK/STAT signal transduction pathway in patients with cancer, Transl Res, 167 (2016) 61 – 6, https://doi.org/10.1016/j.trsl.2015.08.013.

Tables

Table.1 GSEA analysis of MIF in laryngeal carcinoma

Description	setSize	enrichScore	NES	pvalue
KEGG_JAK_STAT_SIGNALING_PATHWAY	155	-0.59	-2.19	0.003
KEGG_ADHERENS_JUNCTION	73	-0.65	-2.11	0.005
KEGG_ARRHYTHMOGENIC_RIGHT_VENTRICULAR_CARDIOMYOPATHY_ARVC	74	-0.65	-2.08	0.007
KEGG_ECM_RECEPTOR_INTERACTION	84	-0.71	-2.03	0.011
KEGG_HUNTINGTONS_DISEASE	180	0.68	2.31	0
KEGG_ALZHEIMERS_DISEASE	165	0.63	2.23	0
KEGG_OXIDATIVE_PHOSPHORYLATION	131	0.78	2.21	0
KEGG_PARKINSONS_DISEASE	128	0.75	2.21	0
KEGG_GLUTATHIONE_METABOLISM	49	0.68	2.11	0.003
KEGG_SPLICEOSOME	127	0.7	2.1	0.003

Figures

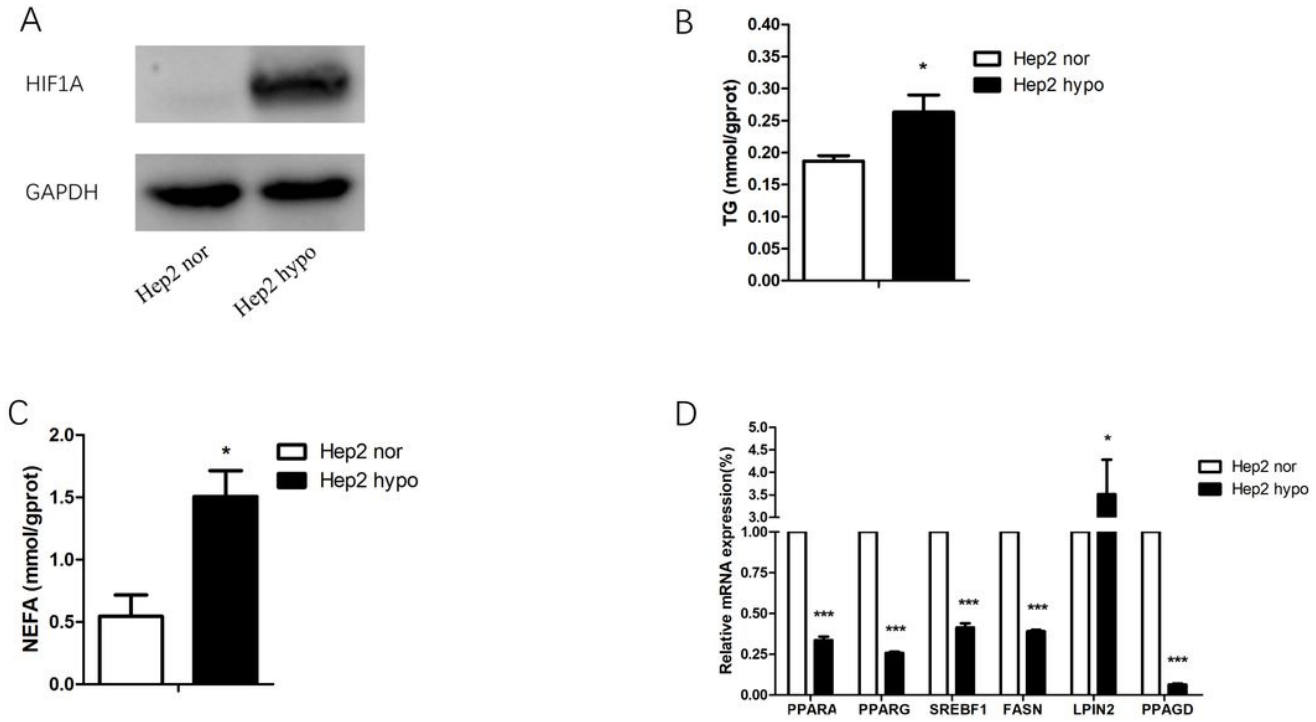

Figure 1

Hypoxia affects lipid metabolism in Hep2 cells. Hep2 cells were treated under hypoxia environment 24h. (A) Protein level of HIF1A were assessed by western blot. (B) TG concentration was assessed by TG assay. (C) NEFA concentration was assessed by NEFA assay. (D) Expressions of lipid metabolism related genes were screened out by. The data are presented as mean ± SD. *p < 0.05; **p < 0.01; ***p < 0.001.

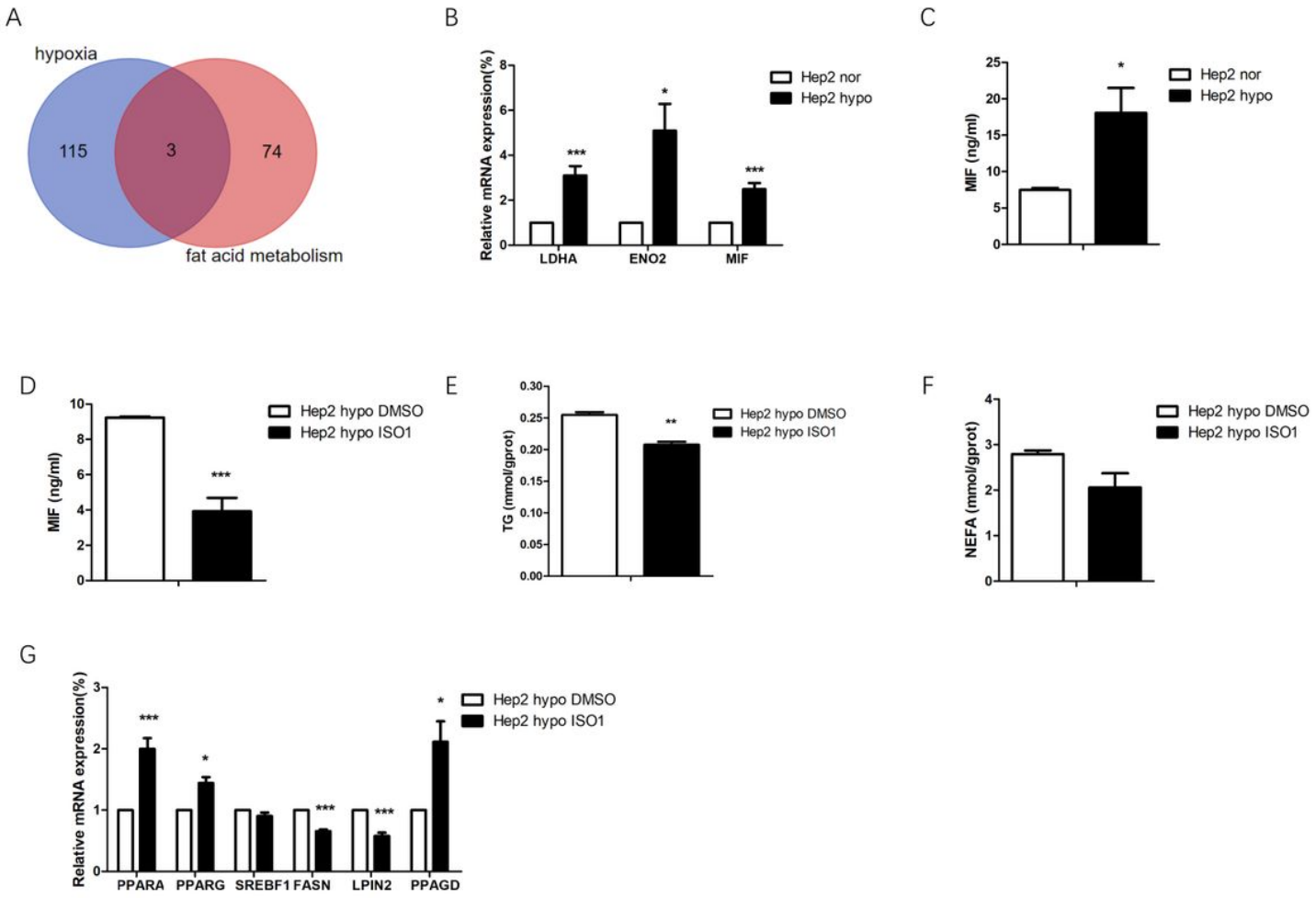

Figure 2

MIF may be a key factor in hypoxia regulating lipid metabolism. (A) Venn diagram showed the intersection of hypoxia gene sets and fatty gene sets. (B) The mRNA expression of MIF, ENO2 and LDHA were verified by qRT-PCR. (C) Protein level of MIF was assessed by ELISA assay. Hep2 cells were treated with 25μM ISO-1. Then MIF protein level(C), TG(D) and NEFA(E) concentration was assessed. The data are presented as mean ± SD. *p < 0.05; **p < 0.01; ***p < 0.001.

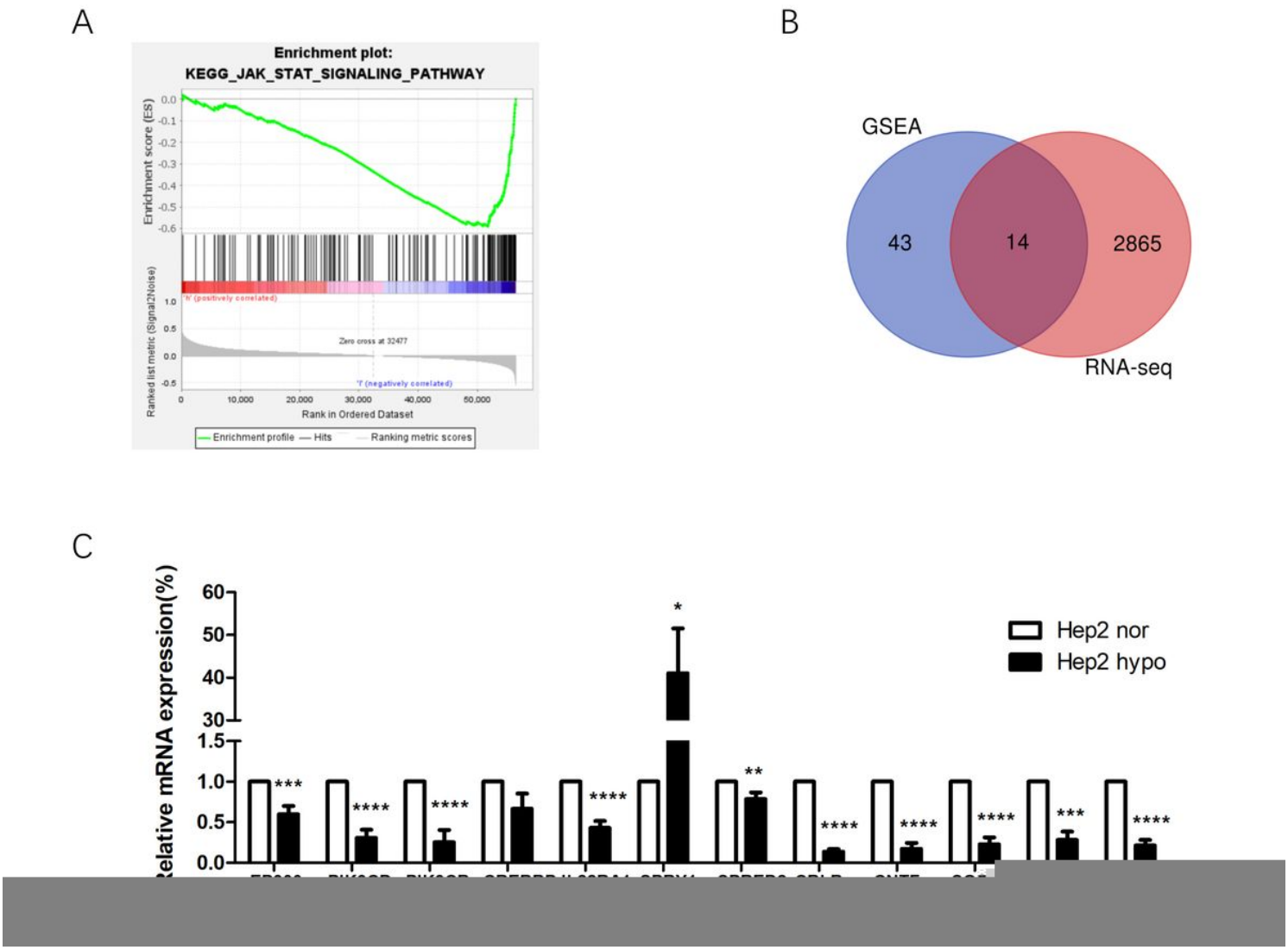

Figure 3

JAK/STAT signaling is involved in MIF regulating pathways in laryngeal cance. (A) GSEA analysis showed JAK/STAT signaling is involved in MIF regulating pathways in laryngeal cance. (B) Venn diagram showed the intersection of JAK/STAT gene sets and differently expressed genes in RNA seq. (C) qRT-PCR showed the intersection gene expression is basically consistent the analysis under hypoxia. The data are presented as mean ± SD. *p < 0.05; **p < 0.01; ***p < 0.001; ****p < 0.0001.

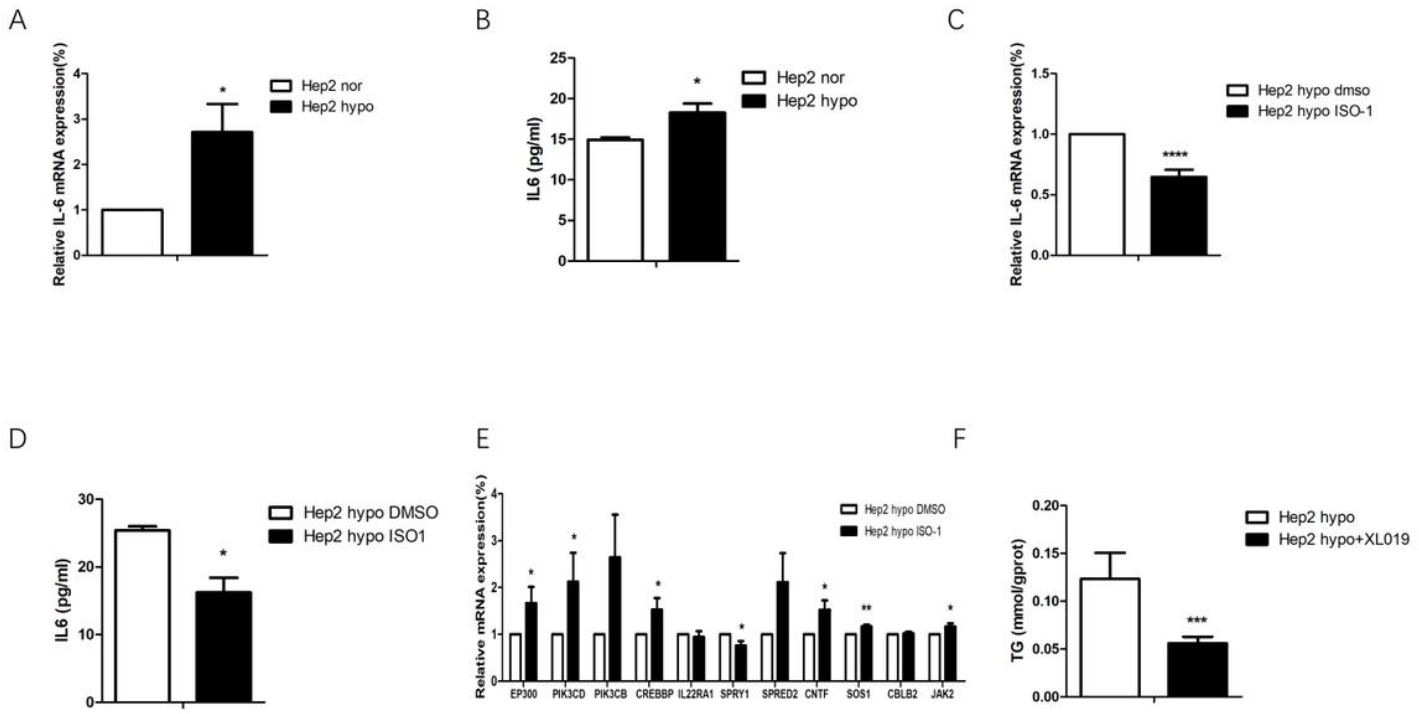

Figure 4

Hypoxia induces MIF regulating lipid metabolism through activating IL-6/JAK/STAT signaling. Hep2 cells were treated with 25μM ISO-1 under hypoxia. Then the mRNA(A) and protein level(B) of IL-6 were assessed by qRT-PCR and western blot. (C)The intersection gene expressions of JAK/STAT gene sets and differently expressed genes in RNA seq were verified. (D) TG concentration of Hep2 cells treated with XL019 or solvent under hypoxia. The data are presented as mean ± SD. *p < 0.05; **p < 0.01; ***p < 0.001.

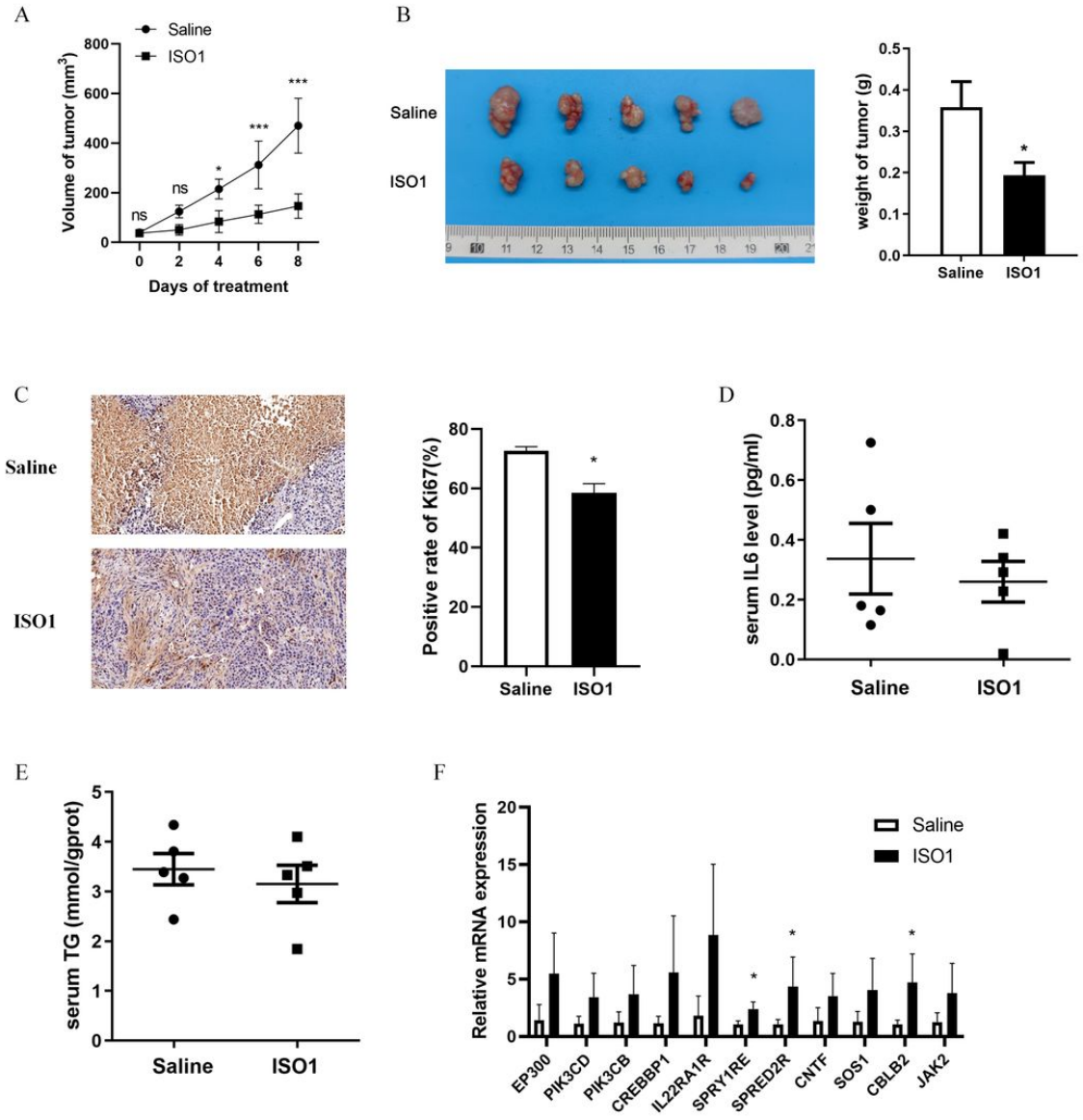

Figure 5

MIF antagonist ISO1 inhibits the tumorigenicity of Hep2 cells in vivo. Four-week-old nude mice (five mice per group) were subcutaneously injected with the Hep2 cells ($4 * 10^6$ cells each mouse) and treated with ISO1 at day eight. (A) The tumor growth curves in vivo. (B) Picture of isolated tumors and tumor weight. (C) Images and statistic results of positive rate of Ki67. (D) Serum IL6 level and (E) serum TG level were assessed by ELISA assay. (F) qRT-PCR was applied to detect relative mRNA expression of JAK/STAT gene sets. The data are presented as mean ± SD. *p < 0.05; **p < 0.01; ***p < 0.001.